JOURNAL OF GUIDANCE, CONTROL, AND DYNAMICS
Vol. 19, No. 1, January–February 1996

Optimization of Generalized Potential in Mission Function Control: Analytical and Experimental Results

Hironori A. Fujii, Masaki Takinami, and Khoichi Matsuda
Tokyo Metropolitan Institute of Technology, Tokyo 191, Japan

The mission function control utilizes the second law of Lyapunov and employs a mission function that is a Lyapunov function, including a hypothetical potential function, generalized potential. The mission function is characterized for its ability to include any functional form of positive-definite generalized potential to complete the control objective. The functional form of the generalized potential is optimized in the sense of minimizing a performance index, and a robust optimal nonlinear and distributed control algorithm for the slew maneuver of flexible structures is presented. The employment of the optimal nonlinear generalized potential naturally achieves improvement of control performance, and it avoids the excessive excitation of the vibration of flexible structures for large attitude angle reorientation in the case of a quadratic generalized potential. The usefulness of the present optimized generalized potential for mission function control is verified both by a numerical simulation and by a hardware experiment.

I. Introduction

CHALLENGING and therefore interesting aspects of control of large flexible space structures (LFSSs) may be summarized by the following two observations.[1,2]

1) LFSSs are described by the distributed parameter system depolying their large structures in space and their structural vibrations with theoretically infinite degrees of freedom cannot expect sufficient numbers of the actuators/sensors nor the ability of the onboard computer to control them.

2) Parameters of LFSSs have uncertainty in their values, being constructed in space under a variable environment, and the control algorithm without sufficient robustness cannot work well.

The observation/control spilover[3] describes the lack of ability in the control of LFSSs caused by the preceding specific features of LFSSs and it is pointed out that such dynamical features as the distributed parameter system must be employed for designing the control algorithm being based on well-posed foundation of models for the LFSSs.[4] In other words, it is not preferable to apply simply

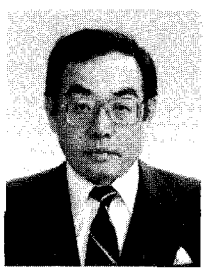

Hironori A. Fujii is a Professor in the Department of Aerospace Engineering at the Tokyo Metropolitan Institute of Technology. He earned his D.E. degree in 1975 from Kyoto University. His research interests include dynamics and control of large space structures and robotics for aerospace application. Since 1982 he has been responsible for the coordination of the Research Group on Control of Flexible Space Structures in Japan. He is an Associate Fellow of AIAA, a member of the American Astronautical Society and the Japan Society for Aeronautical and Space Sciences, and an Associate Fellow of the Canadian Aeronautics and Space Institute.

Masaki Takinami received the B.E. and M.E. degrees in Aerospace Engineering in 1991 and 1993, respectively, from the Tokyo Metropolitan Institute of Technology. He is currently a member of the Technical Staff at Toshiba Electric Corporation. His current research interests include dynamics and control of flexible structures and computation algorithms. He is a Member of AIAA and the Japan Society for Aeronautical and Space Sciences.

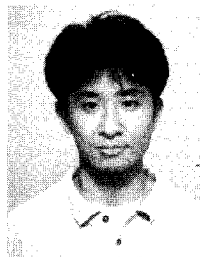

Khoichi Matsuda received the B.E. and M.E. degrees in Aerospace Engineering in 1991 and 1993, respectively, from the Tokyo Metropolitan Institute of Technology. He is currently working towards the Ph.D. degree in Aerospace Engineering at the same institute. His current research interests include dynamics and control of distributed parameter systems. He is a Student Member of AIAA and the Japan Society for Aeronautical and Space Sciences.

Received June 17, 1993; revision received May 10, 1995; accepted for publication May 30, 1995.

the existing control algorithm to a mathematical model of LFSSs being expanded in their vibrational modes and truncated to a finite numbers of flexible modes.

The Lyapunov control method named the mission function control is successfully applied to the slew maneuver of a flexible structure, which is to change the orientation of a spacecraft with suppressing excitation of vibrational motion of flexible structures.[5,6] The usual treatment of the slew maneuver is to employ the truncated modal model of flexible structure and to apply the existing control laws for the model described by the linear state equations of motion resulting in solving the two-point boundary-value problem and thus obtaining open-loop optimal control.[7–11] The mission function control employs the distributed parameter model that is believed to model LFSSs most precisely without any truncation effect and has the feature of an optimal regulator with robustness since the algorithm stands on a well-posed formulation based on the sound dynamical fundamentals as the Lyapunov's direct method.[12] Such treatment of the problem has succeeded by two excellent analyses in consideration of the dynamical feature of the problem: one is treated by Junkins et al.[13] applying the tracking type of control law to furnish the near-minimum-time slew maneuver, and the other is treated by Li and Bainum[14] in consideration of the momentum exchange resulting in an independent flexible control system.

The mission function, or the Lyapunov function, consists of natural energy of the system, e.g., Hamiltonian, and a generalized potential that is added to minimize the function at the desirable object of control. The generalized potential is any positive-definite function and usually selected to be a quadratic form. Junkins et al.[13] have pointed out that such a quadratic form causes an excessive initial actuation since the hypothetical spring to guide the state to the desirable state has maximum force at the initial period of control. This paper is devoted to finding a systematic manner to figure out the functional form of the generalized potential to avoid the excessive initial actuation without assigning such approximation as smooth switch function given a priori being not obtained in an analytic manner.[13]

The generalized potential is optimized by minimizing a performance index concerning the amount of the input force. This procedure has been completed for the application of the Lyapunov control method to the slew maneuver, and the control attains a robust control for the distributed parameter system with an excellent performance. The validity of the control algorithm is examined by an experiment and it is shown that a constraint must be added to stabilize the trajectory of motion to follow the preferable trajectory guided by the optimized generalized potential. Consequently, the excellent performance of the present control algorithm is verified both by numerical analysis and by experiment for the slew maneuver of a flexible structure employing the mission function control, with the optimal generalized potential and resulting in a robust optimum nonlinear and distributed control for LFSSs.

II. System Dynamics and Control Algorithm

System Model

To describe the present analytical procedure, let us focus our attention on one-dimensional attitude motion of a rigid body equipped with a flexible beam, as shown in Fig. 1. The rigid body is actuated by the control torque T_r about the center of rotation C and the flexible beam is deformed by the deflection $v(u, t)$. The flexible beam is assumed to be a Bernoulli–Euler beam with one end ($u = L_0$) fixed on the rigid body and the other end ($u = L$) free. The effect of the air drag is included in the analysis to verify the validity of the analysis compared with the results obtained experimentally on a ground facility. Note that the present analysis can easily be modified to apply to space structures, as has been shown in Refs. 7 and 8. The behavior of the system is described by the following equations of motion (neglecting higher-order terms):

$$I_r\frac{d^2\theta}{dt^2}+\int_{L_0}^{L}\rho u\left(\frac{\partial^2 v}{\partial t^2}+u\frac{d^2\theta}{dt^2}\right)du+\int_{L_0}^{L}cu\left(\frac{\partial v}{\partial t}+u\frac{d\theta}{dt}\right)du=T_r \tag{1}$$

$$\rho\left(\frac{\partial^2 v}{\partial t^2}+u\frac{d^2\theta}{dt^2}\right)+cu\left(\frac{\partial v}{\partial t}+u\frac{d\theta}{dt}\right)+EI\frac{\partial^4 v}{\partial u^4}=0 \tag{2}$$

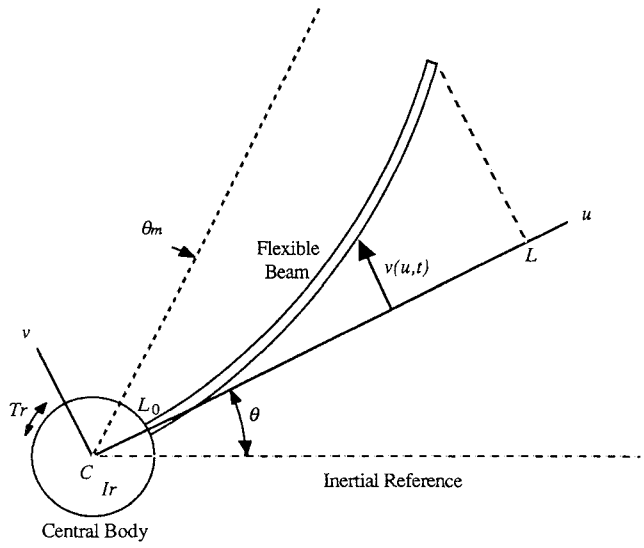

Fig. 1 System model.

with the boundary conditions

$$v=\frac{\partial v}{\partial u}=0\ (u=L_0),\qquad \frac{\partial^2 v}{\partial u^2}=\frac{\partial^3 v}{\partial u^3}=0\ (u=L) \tag{3}$$

where θ, I_r, ρ, EI, and c denote the attitude angle of the central rigid body, the moment of inertia of the central rigid body, the mass density of the beam per unit length, the bending rigidity of the beam, and the damping coefficient of the air drag, respectively. The parameters ρ, EI, and c are assumed to be constant along the beam. The air drag force is assumed to be negative proportional to velocity: $c > 0$.

Mission Function Control Algorithm

The slew maneuver is defined as the transfer of a dynamical system from an initial state with $\theta = \theta_0$ into a desired one (call this desired state the mission state) with

$$\frac{d\theta}{dt}=0,\qquad \theta=\theta_m$$
$$\frac{1}{2}\int_{L_0}^{L}\rho\left(\frac{\partial v}{\partial t}+u\frac{d\theta}{dt}\right)^2du+\frac{1}{2}\int_{L_0}^{L}EI\left(\frac{\partial^2 v}{\partial u^2}\right)^2du=0 \tag{4}$$

where θ_m is the objective attitude angle (call it the mission angle) and the third of Eqs. (4) is the sum of the kinetic energy and the elastic strain energy of the beam.

Let us consider a Lyapunov function, called the mission function, which is positive definite and is zero only at the mission state. The mission function M is defined as

$$M=\frac{a_1}{2}I_r\left(\frac{d\theta}{dt}\right)^2+\frac{a_2}{2}\left[\int_{L_0}^{L}\rho\left(\frac{\partial v}{\partial t}+u\frac{d\theta}{dt}\right)^2du+\int_{L_0}^{L}EI\left(\frac{\partial^2 v}{\partial u^2}\right)^2du\right]+F(\theta) \tag{5}$$

where a_1 and a_2 are positive weighting coefficients and $F(\theta)$ is the positive-definite generalized potential. The first term of Eq. (5) denotes the kinetic energy of a rigid body. The second term of Eq. (5) denotes total energy of the beam, the kinetic energy, and the elastic strain energy. The generalized potential $F(\theta)$ is a positive-definite function of the attitude angle θ, being zero only at $\theta = \theta_m$, and is assumed to be in an arbitrary functional form in the present paper.

Selecting the control torque T_r as

$$T_r=-\frac{1}{a_1}\left[a_3\frac{d\theta}{dt}-(a_2-a_1)(M_0-L_0S_0)+\phi(\theta)\right] \tag{6}$$

where M_0 and S_0 denote the bending moment and the shearing force at the root of the beam, respectively, and $\phi(\theta)$ denotes the derivative of the generalized potential $F(\theta)$ with respect to the attitude angle θ, that is, $\phi = \mathrm{d}F/\mathrm{d}\theta$ and using Eqs. (1–3), the time derivative of the mission function is obtained through the trajectory of motion as

$$\frac{\mathrm{d}M}{\mathrm{d}t} = -a_3\left(\frac{\mathrm{d}\theta}{\mathrm{d}t}\right)^2 - a_2 c\int_{L_0}^{L}\left(\frac{\partial v}{\partial t} + u\frac{\mathrm{d}\theta}{\mathrm{d}t}\right)^2 \mathrm{d}u \tag{7}$$

The time derivative of the mission function is apparently negative semidefinite and it is shown that the mission state is asymptotically stable in the sense of Lyapunov. This expression of the torque, Eq. (6), is used as a control algorithm for the slew maneuver treated in this paper. Note that the control algorithm is derived directly from the partial differential equations that describe the distributed parameter system most precisely without any crucial truncation effect,[15] and it is naturally evident that sufficient data to simultaneously control the rotary motion of the central rigid body and vibration of the cantilever beam are contained in the hub rotational state (θ, $\mathrm{d}\theta/\mathrm{d}t$), the bending moment ($M_0$), and the shear force ($S_0$) at the root of the flexible beam.

As is evident from Eq. (6), the generalized potential $F(\theta)$ appears as the input torque in the form of the derivative ϕ of $F(\theta)$ with respect to θ, and the derivative ϕ is examined for its optimal value through optimization of a performance index to design the present control algorithm.

III. Optimization of Generalized Potential

Excessive initial actuation in flexible structural vibration for large attitude reorientation is undesirable when the mission function control employs the quadratic generalized potential,[5,6] i.e.,

$$F = \tfrac{1}{2}a_f(\theta - \theta_m)^2 \tag{8}$$

with its derivative with respect to attitude angle

$$\phi = a_f(\theta - \theta_m) \tag{9}$$

as pointed out by Junkins et al.[13] and it is necessary to figure out a nonlinear generalized potential in a systematic approach for large attitude reorientation to achieve good performance of the mission function control. The systematic approach means the generalized potential is determined from an optimal control formulation with any prescribed performance index. Note that the smoothing of any switching function[13] is not formulated through any optimal control formulation, although the generic switching function is the solution of the optimal time control.

This paper formulates the optimal mission function control in such a systematic manner as to optimize the functional form of the generalized potential contained in the mission function through employing a performance index. The rest of this section is devoted to describing a procedure to obtain the optimized mission function control algorithm with such an excellent performance as a hybrid of both the preferable features of the mission function control and the linear quadratic regulator, which leads to a robust optimal nonlinear and distributed control algorithm.

Optimization Without Inequality Constraint

A modal model is utilized in the procedure of optimizing the generalized potential. Note that the system is modeled as a distributed parameter system in the fundamental design of the present controller and is thus free from the crucial truncation effect without regard to utilization of the modal model to obtain the functional form of the generalized potential.

The equations of motion (1) and (2) can be discretized and reduced to the following standard form, expanding the vibrational flexible motion by the superposition of the constrained mode[16] with the truncation number N:

$$M'\ddot{\eta} + D'\dot{\eta} + K'\eta = b'T_r, \qquad \eta = \left[(\theta - \theta_m)q^T\right]^T \tag{10}$$

with $(\cdot) = \mathrm{d}(\,)/\mathrm{d}t$, where q denotes an N-dimensional vector of the cantilever modal coordinates; the $(N+1)\times(N+1)$ matrices M', D', and K' are mass, damping, and stiffness matrices, respectively; and the $(N+1)$-dimensional vector $b' = [1\ \ 0\cdots 0]^T$. The constrained mode model, Eq. (10), is transformed into the unconstrained mode model[16] by the coordinate transformation $\eta = Q\zeta$:

$$\ddot{\zeta} + D\dot{\zeta} + K\zeta = bT_r \tag{11}$$

where the $(N+1)\times(N+1)$ matrix Q is a transformation matrix with $M' = (Q^{-1})^T Q^{-1}$, $D = Q^T D' Q$, $K = Q^T K' Q$, and $b = Q^T b'$. The matrix Q can be obtained by Cholesky or eigenvalue decompositions of the matrix M'. The state equation then becomes

$$\dot{s} = \tilde{A}s + \tilde{B}T, \qquad s^T = [\zeta^T \quad \dot{\zeta}^T] \tag{12}$$

where

$$\tilde{A} = \begin{bmatrix} O_{N+1} & I_{N+1} \\ -K & -D \end{bmatrix}, \qquad \tilde{B} = [0\cdots 0 \quad b^T]^T$$

and the matrices O_{N+1} and I_{N+1} are $(N+1)\times(N+1)$ null and unit matrices, respectively. The mission function control torque, Eq. (6), is represented in the state space model by the following form:

$$T_r = -K_1 s - K_2\phi(\theta) \tag{13}$$

where K_1 is an $(N+1)$-dimensional row vector that is derived from the transfer matrices between sensor outputs, θ and $M_0 - L_0 S_0$, and the state s, and $K_2 = 1/a_1$. Note that the derivative of the generalized potential ϕ is formulated as a nonlinear feedback term of the attitude angle θ in the present analysis to accommodate large attitude angle reorientation.

An optimal terminal control problem is formulated to minimize the following performance index, which is a quadratic form of the control input T_r:

$$J = \frac{1}{2}\int_{t_0}^{t_f} T_r^2\,\mathrm{d}t \tag{14}$$

with the boundary conditions

$$\begin{aligned} s(t = t_0) &= s_0 = [-\theta_m/Q_{11} \quad 0\cdots 0]^T \\ s(t = t_f) &= s_f = [0\cdots 0]^T \end{aligned} \tag{15}$$

where t_0 and t_f are initial and terminal times, respectively, in the control strategy and Q_{11} is the (1, 1) element of the matrix Q. The terminal time is fixed and the terminal state is constrained to zero. This linear quadratic (LQ) terminal control problem is solved by using a transition matrix.

The derivative of the generalized potential is represented from Eq. (13) in the following form:

$$\phi = -(1/K_2)(T_r + K_1 s) \tag{16}$$

and the attitude angle θ is represented by the state s as follows:

$$\theta = C_\theta s + \theta_m \tag{17}$$

where $C_\theta = b'^T Q[I_{N+1} \quad O_{N+1}]$. The derivative ϕ and attitude angle θ are solved from the solutions s and T_r of the optimal control problem and obtained as a time history. The optimal derivative ϕ is thus determined numerically as a function of the attitude angle θ and is a nonlinear function processed numerically being optimal for large attitude angle reorientation.

The generalized potential F is determined from the definition as follows:

$$F(\theta) = \int_{\theta_0}^{\theta}\phi(\xi)\,\mathrm{d}\xi + F(\theta_0) \tag{18}$$

where the derivative ϕ is integrated numerically with respect to the attitude angle θ through Simpson's rule.

Stability of the Optimal Trajectory About the Attitude Angle (Robustness)

In general, performance and stability robustness are required for implementation of designed controllers due to inevitable modeling error of real systems. Let us consider stability of the optimal trajectory about the deviation of the attitude angle. The third term, T_{r3}, in Eq. (6) is only dependent on the attitude angle θ as

$$T_{r3} = -(1/a_1)\phi(\theta) \tag{19}$$

A variation of Eq. (19) with respect to the attitude angle θ gives

$$\delta T_{r3} = -\frac{1}{a_1}\frac{\mathrm{d}\phi}{\mathrm{d}\theta}\delta\theta \tag{20}$$

where $\delta(\,)$ denotes the variation of $(\,)$. It is easily seen that when $\mathrm{d}\phi/\mathrm{d}\theta$ is negative, the spring coefficient becomes negative, and then the optimal trajectory is unstable about the variation of the attitude angle $\delta\theta$. Thus the system should satisfy the following inequality condition to guarantee the stability of the optimal trajectory:

$$\frac{\mathrm{d}\phi}{\mathrm{d}\theta} > 0 \tag{21}$$

It may be noted that $\mathrm{d}\phi/\mathrm{d}\theta$ has a positive constant a_f, and thus the stability is guaranteed by using the quadratic generalized potential in Eq. (8).

Optimization with Inequality Constraint

To add the inequality condition, Eq. (21), to the present optimal control problem, the inequality condition is transformed into the following time-derivative form:

$$\frac{\mathrm{d}\phi}{\mathrm{d}\theta} = \frac{\mathrm{d}\phi/\mathrm{d}t}{\mathrm{d}\theta/\mathrm{d}t} = \frac{\dot{\phi}}{\dot{\theta}} > 0 \tag{22}$$

Multiplied by the squared angular velocity, the inequality condition, Eq. (22), is then transformed as follows:

$$S_i = \dot{\phi}\dot{\theta} > 0 \tag{23}$$

where $\dot{\phi}$ is obtained from the time derivative of Eq. (16):

$$\dot{\phi} = -(1/K_2)(\dot{T}_r + K_1\dot{s}) \tag{24}$$

The angular velocity $\dot{\theta}$ is obtained from Eq. (12) as

$$\dot{\theta} = C_{\dot{\theta}}s \tag{25}$$

where $C_{\dot{\theta}} = b'^T Q[O_{N+1} \;\; I_{N+1}]$. The inequality condition (21) to guarantee stability of the optimal trajectory is transformed into the following form:

$$S_i = -(1/K_2)(\dot{T}_r + K_1\dot{s})C_{\dot{\theta}}s > 0 \tag{26}$$

which is transformed into the following equality constraint using a dummy control input u_d:

$$S(x,u) = S_i - \tfrac{1}{2}u_d^2 = 0 \tag{27}$$

The preceding manipulations are summarized in terms of the state–input relation

$$\dot{x} = \begin{bmatrix} \tilde{A} & \tilde{B} \\ 0 & 0 \end{bmatrix} x + \begin{bmatrix} 0 & 0 \\ 1 & 0 \end{bmatrix} u = Ax + Bu \tag{28}$$

defining the state and the input as

$$x = \begin{bmatrix} s \\ T_r \end{bmatrix}, \qquad u = \begin{bmatrix} \dot{T}_r \\ u_d \end{bmatrix} \tag{29}$$

and the constraint (27),

$$S(x,u) = -(1/K_2)(\dot{T}_r + K_1'x)C_{\dot{\theta}}'x - \tfrac{1}{2}u_d^2 = 0 \tag{30}$$

where $K_1' = K_1Y$, $C_{\dot{\theta}}' = C_{\dot{\theta}}Y$, and $Y = [I_{2(N+1)}\;[0\cdots 0]^T]$.

The performance index of the present optimal control problem is defined as follows:

$$J = \frac{1}{2}\int_{t_0}^{t_f}\left[\dot{T}_r^2 + r\dot{T}_r^2\right]\mathrm{d}t = \frac{1}{2}\int_{t_0}^{t_f}[x^T Wx + u^T Ru]\,\mathrm{d}t \tag{31}$$

with the boundary conditions

$$x_0 = \begin{bmatrix} s_0 \\ T_{r0} \end{bmatrix}, \qquad x_f = \begin{bmatrix} s_f \\ T_{rf} \end{bmatrix} \tag{32}$$

where s_0 and s_f are given; $T_{r0} = T_r(t=0)$ and $T_{rf} = T_r(t=t_f)$ are free, which imposes constraints on the adjoint variable; r is a positive small coefficient; $W = \mathrm{diag}[0,\ldots,0,1]$; and $R = \mathrm{diag}[r,0]$. The integral of the squared time derivative of the control torque is added to the performance index to avoid numerical difficulties and to improve the stability of numerical processing. The problem results in a nonlinear two-point boundary-value problem in which the initial conditions are partially free. The modified quasilinearization algorithm[17] is a numerical second-order method to solve optimal control problems and is employed to solve the present problem.

As the results, the optimal generalized potential F and its derivative ϕ are obtained and found through use of Eqs. (16–18) completing the robust optimal nonlinear and distributed control algorithm.

IV. Experiment Setup

The diagram of experimental setup is shown in Fig. 2. The flexible beam employed in this experiment is a 1.189-m-long aluminum beam with a cross section of $(20.0 \times 10^{-3}) \times (0.50 \times 10^{-3})$ m. The model parameters are shown in Table 1. The model is set on a zero-gravity simulation table and allowed to move free from gravity of the Earth. The surface of the table is made of porous metal with many tiny holes and the air flows from these holes to float a specimen on the table. The model beam is equipped with three 0.145-m-diam circular boards made of styrene resin to receive the airflow and to move freely in the horizontal plane. Note the ith modal frequency ω_i of the flexible vibration, $\omega_1 = 0.3$ Hz, $\omega_2 = 1.2$ Hz, and $\omega_3 = 4.0$ Hz.

The control loop diagram in the present experiment is shown in Fig. 3. Sensing is provided by a tachometer at the rotary shaft of the torque motor and two bridge strain gauges located at the root of the beam to obtain the necessary data for the control. The tachometer is used to measure angular rate of the central rigid body about the rotary axis, and its output is integrated by an analog circuit to obtain the attitude angle of the central rigid body. The strain gauges are used to measure bending moment and shear force at the root of the beam. Data from these sensors are amplified and put

Table 1 Model parameters

Central body
$I_r = 3.43 \times 10^{-2}$ kg · m^2
$I_f/I_r = 0.95$
Flexible appendage
$L = 1.189$ m
$L_0 = 33.8 \times 10^{-3}$ m
$EI = 1.47 \times 10^{-2}$ N · m^2
$\rho = 5.84 \times 10^{-2}$ kg/m
$c = 1.10 \times 10^{-2}$ N · s/m^2
$I_f = 3.27 \times 10^{-2}$ kg · m^2 [a]

[a] Moment of inertia of the undeformed appendage about the spin axis, nearly coincident with the center of mass of the total system.

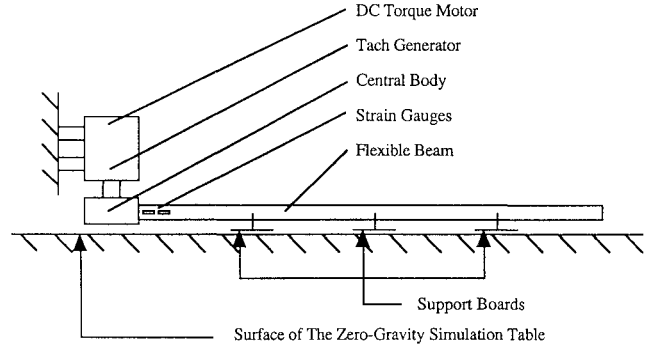

Fig. 2 Diagram of experimental setup.

Table 2 Control performance

Case	Fig.	Conditions	Initial angle, $\theta_0 \times 10^{-2}$ rad	Initial torque, $T_r(t_0)$, N·m	Maximum amplitude, $M_0 - L_0S_0 \times 10^{-3}$ N·m	Performance index, $J = \int T_r^2\,dt$
1a	6	Quadratic form	0	0.157	−14.1	1.60
1b	7	Without inequality constraints	0	0.017	−11.0	0.40
1c	8	With inequality constraints	0	0.129	−13.2	1.36
2b	9	Without inequality constraints	8.73	0.101	−13.3	0.86
2c	10	With inequality constraints	8.73	0.131	−13.9	1.20

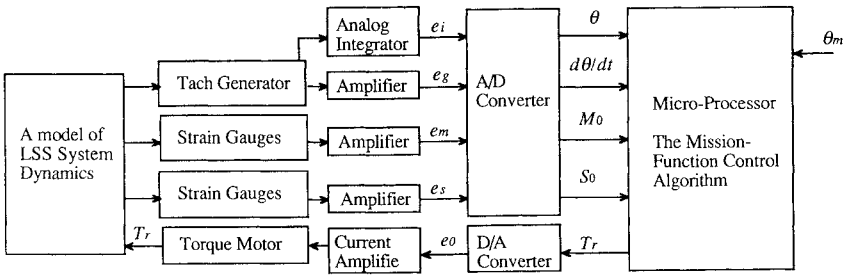

Fig. 3 Control loop diagram.

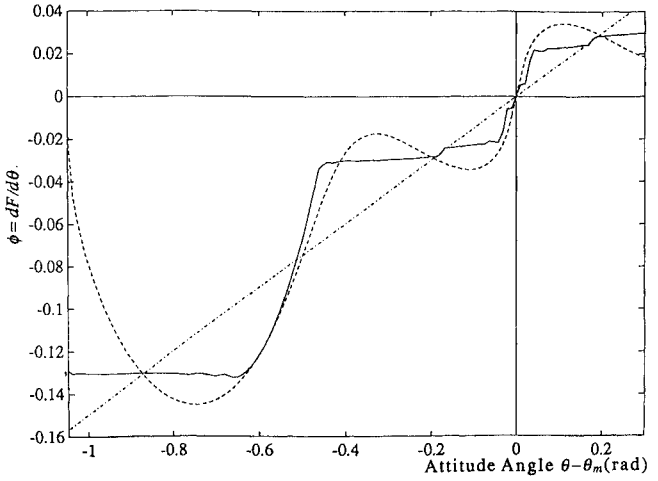

Fig. 4 Configuration of the derivative of the generalized potential: – · – · –, case a; - - -, case b; and ——, case c.

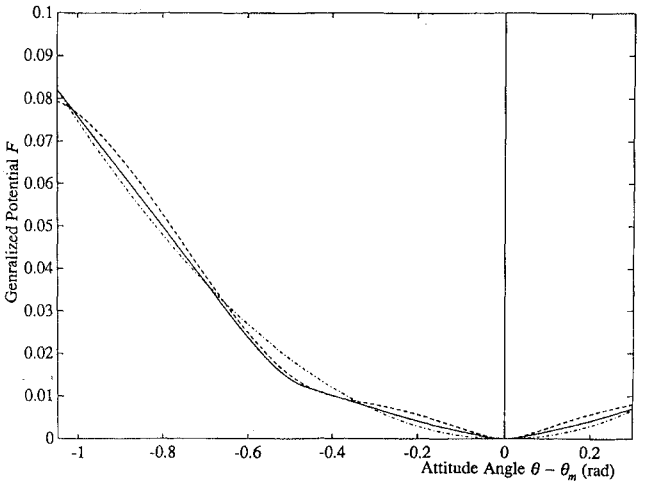

Fig. 5 Configuration of the generalized potential: – · – · –, case a; - - -, case b; and ——, case c.

into a digital computer, NEC PC-9801VM (CPU:8086), through an analog-to-digital (A/D) converter. The computer processes the data under the control algorithm and outputs a control signal to drive the torque motor through a digital-to-analog (D/A) converter. The control signal is converted to electric current by a current amplifier to drive the motor. The sample interval of the control process is set to be 10.0 ms.

V. Results of Numerical Simulation and Experiment

The model is controlled to slew from $\theta_0 = 0$ to $\theta_m = \pi/3$ rad (60.0 deg). The value of the weighting coefficients a_1, a_2, and a_3 are selected as 1.00, 5.14, and 2.76 N·m·s, respectively. In the procedure of optimizing the generalized potential, the modal model is truncated higher than the first order with its natural frequency of about 0.3 Hz in Eq. (11), the terminal time is fixed to 5 s, and the weighting coefficient of the performance index r is set to be 0.01. The system responses are simulated numerically through applying the finite difference method with 20 finite elements for the flexible beam (approximately retaining up to 16 flexible modes) to the partial differential equations, Eqs. (1–3).

In the present experiments, the initial angle θ_0 is set to be 1) the nominal value of 0 rad and also to be 2) 8.73×10^{-2} rad (5.00 deg) to introduce parameter uncertainties or disturbances into the model.

In the numerical simulations and hardware experiments, three kinds of the generalized potential are employed: a quadratic form case a, and optimized without, case b, and with, case c, the inequality constraint. Figure 4 shows the derivative ϕ of the generalized potential with respect to the artitude angle θ in three cases a–c. The generalized potential F is shown in Fig. 5. The derivative ϕ denotes a nonlinear feedback term of the attitude angle θ in the control torque T_r (a linear one in the case a). As is pointed out already, the large initial torque is seen to introduce an excessively large transient response of the flexible structure in the quadratic generalized potential of case a.

Five cases, 1a–1c, 2b, and 2c, are experimentally demonstrated as the combination of the preceding initial conditions, 1 and 2, and the three functional forms of F. The results of these five cases are shown in Figs. 6–10 denoting time responses of the attitude angle θ, the angular velocity of the rigid body $\dot{\theta}$, the moment at the root of the beam $(M_0 - L_0S_0)$, and the control torque T_r, respectively. Table 2 summarizes some typical features of the control performance under various conditions in the experiments. The maximum amplitude of the moment $(M_0 - L_0S_0)$ can be considered a measure of the intensity of vibrational excitation in the flexible beam. The performance index J is computed by integrating the squared control torque numerically through Simpson's rule.

Results of Case 1: Initial Angle $\theta_0 = 0$ rad

Figures 6–8 show the results of the cases 1a–1c, respectively. Compared with case 1a, the quadratic generalized potential, the control performance of case 1b is improved, i.e., 89% in the initial torque Tr_0, 22% in the maximum amplitude of the moment $(M_0 - L_0S_0)$, and 75% in the performance index J. The control performance of case 1c is improved 18% in the initial torque T_{r0}, 6% in the maximum amplitude of the moment $(M_0 - L_0S_0)$, and

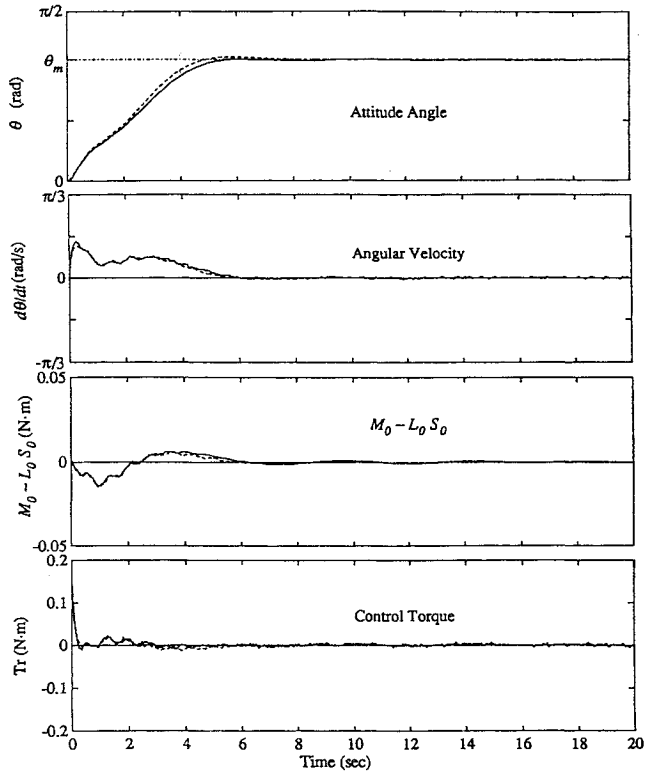

Fig. 6 Time response, case 1a, quadratic generalized potential: ——, experiment; and - - -, numerical simulation.

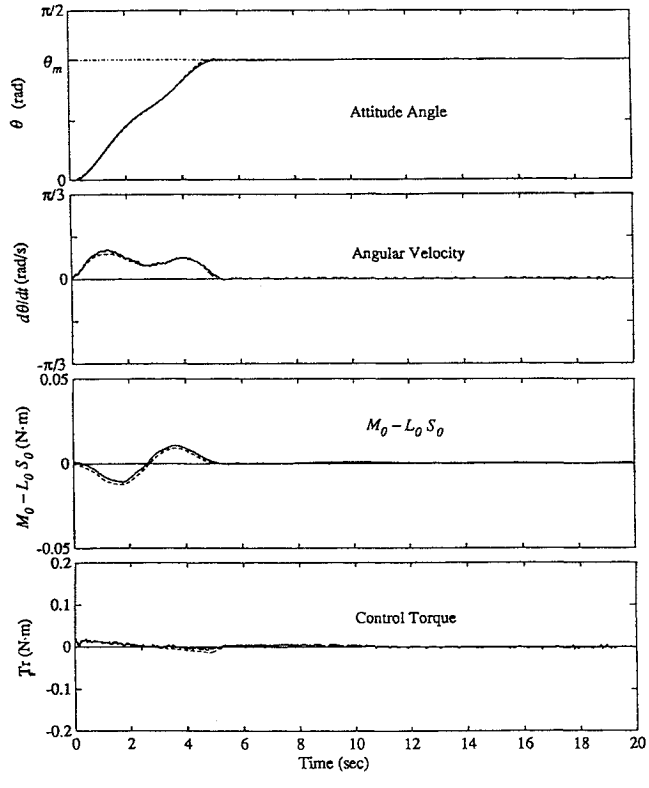

Fig. 7 Time response, case 1b, optimizing without inequality constraint: ——, experiment; and - - -, numerical simulation.

15% in the performance index J. These three control performance indices are improved by optimizing the generalized potential with and without the inequality constraint, compared with that of the usual quadratic form.

Results of Case 2: Initial Angle $\theta_0 = 8.73 \times 10^{-2}$ rad (5.00 deg)

To introduce parameter uncertainties or disturbances into the model, the initial attitude angle θ_0 is deviated by about 8% of

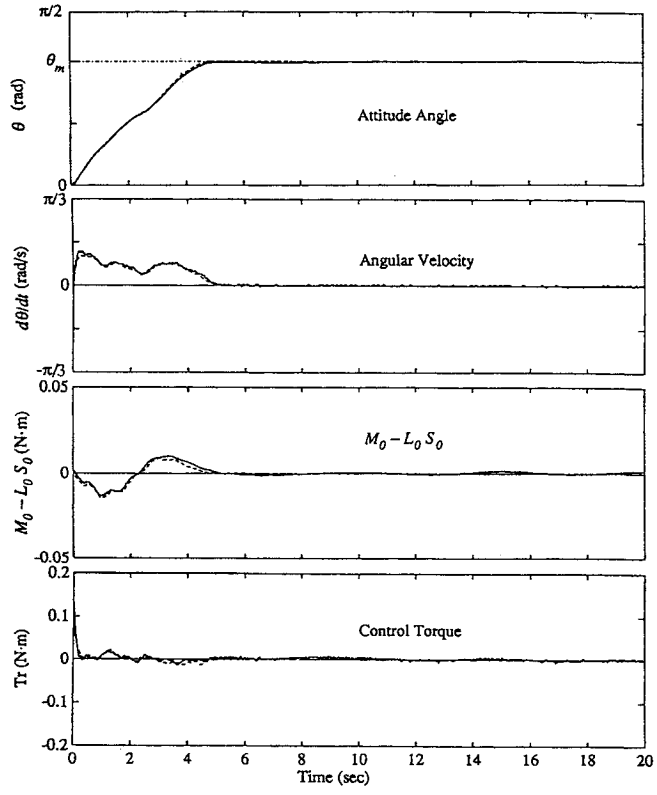

Fig. 8 Time response, case 1c, optimizing with the inequality constraint: ——, experiment; and - - -, numerical simulation.

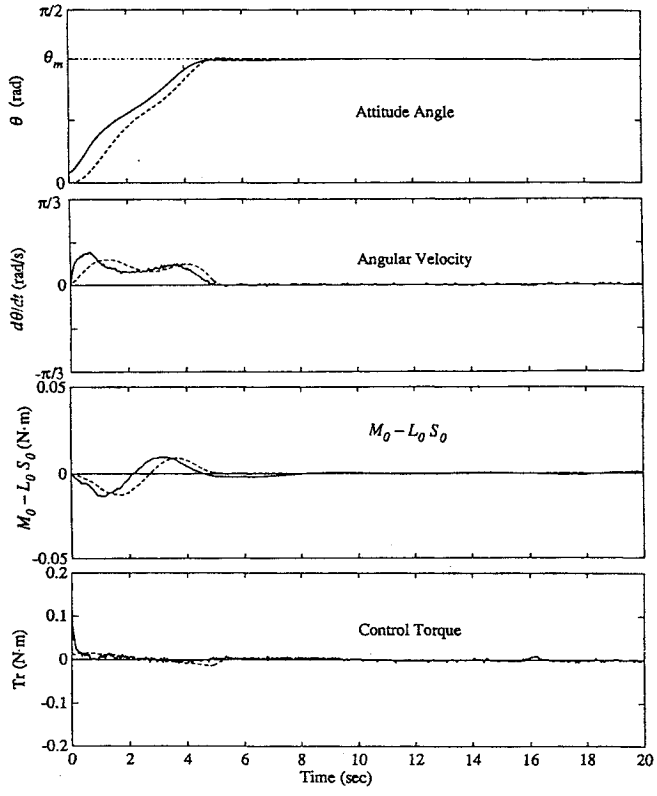

Fig. 9 Time response, case 2b, optimizing without inequality constraint: ——, experiment; and - - -, numerical simulation.

the mission angle and set to be 8.73×10^{-2} rad (5.00 deg). The generalized potential is optimized without the inequality constraint in case 2b, and Fig. 9 shows that the trajectory never approaches the optimal trajectory and attains the mission state through a path different from the optimal trajectory. The control performance clearly becomes much worse than that of case 1b as shown in Table 2. In case 2c, the generalized potential is optimized with the inequality

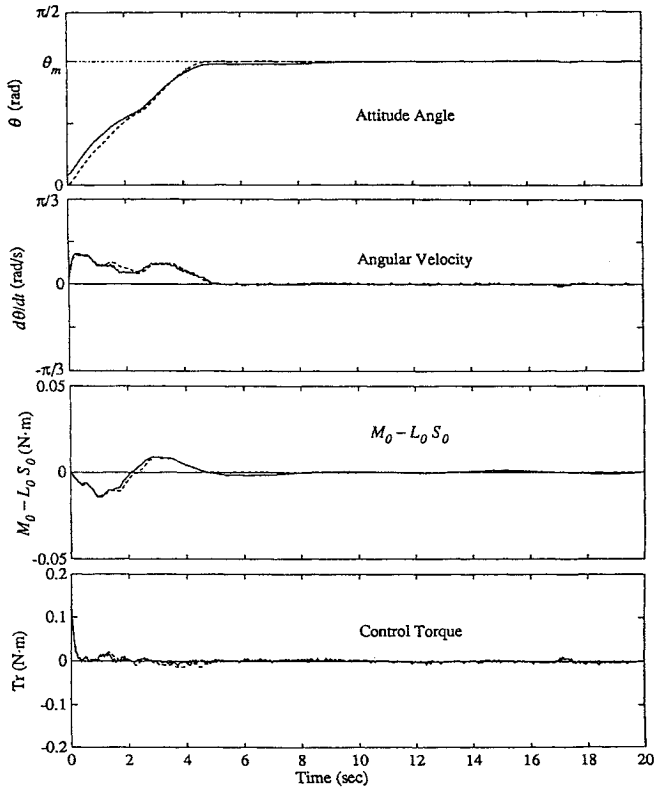

Fig. 10 Time response, case 2c, optimizing with the inequality constraint: ——, experiment; and - - -, numerical simulation.

constraint, which guarantees stability of the optimal trajectory, and Fig. 10 shows that the trajectory in the experiment approaches and overlaps the optimal trajectory as time increases.

Some typical features of the control performance are compared 1) without and 2) with deviations in the initial angle. In case 2b, the initial torque T_{r0} becomes 5.94, the maximum amplitude of the moment $(M_0 - L_0 S_0)$ 1.21, and the performance index J 2.15 times as large as that of case 1b, and the control performance is seen to become worse in this case. In this case, the initial torque at the slew maneuver, which is equal to the value of the generalized potential at the initial angle, is reduced to about 10% of those of other cases. The gradient of the derivative of the generalized potential is, however, negative at the initial angle in the case of the optimized generalized potential without the inequality constraint as shown in Fig. 4; then the optimal trajectory becomes unstable. The control performance becomes worse to pass a different trajectory from the optimal trajectory through the introduction of parameter error.

Notable differences are not found in the initial torque T_{r0} and the maximum amplitude of the moment $(M_0 - L_0 S_0)$ between cases 1c and 2c. The performance index J is reduced by 12% for the case with the deviation in the initial angle. The present control law with the generalized potential c is thus concluded to have robust features concerning the parameter uncertainties of the model, resulting in the robust optimal nonlinear and distributed control algorithm.

VI. Conclusions

The generalized potential of the mission function is optimized in the sense of minimizing the integral of the squared control torque. The mission function control is optimized and guarantees the asymptotic stability for the distributed parameter system. The control performance is improved by employing the optimal generalized potential in comparison with the quadratic generalized potential concerning the maximum control torque and the excessive vibrational excitation in the flexible structure.

A constraint is added in the optimization of the generalized potential to guarantee the stability of trajectory of motion around the optimal trajectory and the control is proven to have robust features concerning parameter uncertainties or disturbances of the model. The resulting control law is a robust-optimal nonlinear and distributed control algorithm for large space structures.

These favorable features of the control performance presented in this paper are verified both by the on-ground experiment and by the numerical simulation.

Acknowledgment

The authors sincerely appreciate the helpful advice of T. Ohtsuka during the development of this work.

References

[1]Nurre, G. S., Ryan, R. S., Scofield, H. N., and Sims, J. L., "Dynamics and Control of Large Space Structures," *Journal of Guidance, Control, and Dynamics*, Vol. 7, No. 5, 1984, pp. 514–526.

[2]Spark, D. W., Jr., and Juang, J.-N., "Survey of Experiments and Experimental Facilities for Control of Flexible Structures," *Journal of Guidance, Control, and Dynamics*, Vol. 15, No. 4, 1992, pp. 801–816.

[3]Schaechter, D. B., "Hardware Demonstration of Flexible Beam Control," *Journal of Guidance, Control, and Dynamics*, Vol. 5, No. 1, 1982, pp. 48–53.

[4]Oz, H., "Control of Flexible Systems and Principles of Structural Mechanics," AIAA Paper 84-2001, Aug. 1984.

[5]Fujii, H., and Ishijima, S., "Mission-Function Control for Slew Maneuver of a Flexible Space Structure," *Journal of Guidance, Control, and Dynamics*, Vol. 12, No. 6, 1989, pp. 858–865.

[6]Fujii, H., Ohtsuka, T., and Udou, S., "Mission-Function Control for a Slew Maneuver Experiment," *Journal of Guidance, Control, and Dynamics*, Vol. 14, No. 3, 1991, pp. 986–992.

[7]Turner, J. D., and Junkins, J. L., "Optimal Large-Angle Single-Axis Rotational Maneuver of Flexible Spacecraft," *Journal of Guidance and Control*, Vol. 3, No. 6, 1980, pp. 578–585.

[8]Breakwell, J. A., "Optimal Feedback Slewing of Flexible Spacecraft," *Journal of Guidance and Control*, Vol. 4, No. 5, 1981, pp. 472–479.

[9]Juang, J.-N., Horta, L. G., and Robershaw, H. H., "A Slewing Control Experiment for Flexible Structures," *Journal of Guidance, Control, and Dynamics*, Vol. 9, No. 5, 1986, pp. 599–607.

[10]Kida, T., Yamaguchi, I., Ohkami, Y., Hirako, K., and Soga, H., "An Optimal Slewing Maneuver Approach for a Class of Spacecraft with Flexible Appendages," *Acta Astronautica*, Vol. 13, No. 6/7, 1986, pp. 311–318.

[11]Bikdash, M., Cliff, E. M., and Nayfeh, A. H., "Closed-Loop Soft-Constrained Time-Optimal Control of Flexible Space Structures," *Journal of Guidance, Control, and Dynamics*, Vol. 15, No. 1, 1992, pp. 96–103.

[12]Fujii, H., "A Feature of the MF (Mission-Function) Control," *Transactions of the Japan Society for Aeronautical and Space Sciences*, Vol. 35, No. 107, 1992, pp. 14–26.

[13]Junkins, J. L., Rahman, Z. H., and Bang, H., "Near-Minimum-Time Maneuvers of Flexible Vehicles: Analytical and Experimental Results," *Journal of Guidance, Control, and Dynamics*, Vol. 14, No. 2, 1991, pp. 406–415.

[14]Li, Z., and Bainum, P. M., "Momentum Exchange: Feedback Control of Flexible Spacecraft Maneuvers and Vibrations," *Journal of Guidance, Control, and Dynamics*, Vol. 15, No. 6, 1992, pp. 1345–1360.

[15]Hughes, P. C., "Space Structure Vibration Modes: How Many Exist? Which Ones are Important?" Inst. for Aerospace Studies, Univ. of Toronto, UTIAS TN 252, Toronto, ON, Canada, June 1984.

[16]Hablani, H. B., "Constrained and Unconstrained Modes: Some Modeling Aspects of Flexible Spacecraft," *Journal of Guidance, Control, and Dynamics*, Vol. 5, No. 2, 1982, pp. 164–173.

[17]Gonzalez, S., and Rodriguez, S., "Modified Quasilinearization Algorithm for Optimal Control Problems with Nondifferential Constraints and General Boundary Conditions," *Journal of Optimization Theory and Applications*, Vol. 50, No. 1, 1986, pp. 109–128.